processes

MDPI

Article

Study on the Influence of Working Characteristics of Centripetal Pump Based on VOF/Mixture Model

Shoulie Liu [1], Hefeng Dong [2], Shaobin Li [1,*] and Xizhen Song [1]

[1] School of Energy and Power Engineering, Beijing University of Aeronautics and Astronautics, Beijing 101191, China; liushoulie@163.com (S.L.)
[2] Systems Engineering Research Institute, China State Shipbuilding Corporation Limited, Beijing 100194, China
* Correspondence: lee_shaobin@buaa.edu.cn

Abstract: Aviation fuel contamination can seriously affect aircraft flight safety, and the centripetal pump is the core component of aviation fuel purification equipment. The performance of centripetal pumps is highly demanded for purification equipment. The operating parameters of centripetal pumps significantly affect the internal flow characteristics, which affects the performance of centripetal pumps. However, the flow characteristics of a centripetal pump influenced by the operating parameters have not yet been elaborated upon. In this research, a three-dimensional numerical simulation of the air-fuel two-phase flow field inside a centripetal pump was carried out using the VOF/Mixture model to investigate the effects of three relatively independent physical quantities, namely, fuel flow, outlet fuel discharge pressure, and rotational speed, on the operating characteristics of the centripetal pump. The flow law inside the flow channel of a centripetal pump was analyzed based on a rotating fluid pressure model, the free liquid surface radius of air-fuel, and the total pressure recovery coefficient. It was found that centripetal pumps have a steady working state and an unsteady working state. In a steady working state, the proportion of separated zones in the flow channel of the centripetal pump is small, the flow coefficient *C* of the flow channel is greater than 1, and the total pressure recovery coefficient of the centripetal pump is high. In an unsteady working state, the separation zone in the flow channel of the centripetal pump accounts for a large proportion, the flow channel flow coefficient *C* is less than 1, and the total pressure recovery coefficient of the centripetal pump is low. An unsteady working state can easily occur in small flow, high-speed conditions. By analyzing the working state and flow characteristics of the centripetal pump, the mechanism of the influence of the flow, outlet fuel discharge pressure, and rotational speed on the working state of the centripetal pump is revealed, which provides a basis for the stable operation of the centripetal pump.

Keywords: centripetal pump; working characteristics; two-phase flow; numerical simulation

Citation: Liu, S.; Dong, H.; Li, S.; Song, X. Study on the Influence of Working Characteristics of Centripetal Pump Based on VOF/Mixture Model. *Processes* **2024**, *12*, 1376. https://doi.org/10.3390/pr12071376

Academic Editor: Blaž Likozar

Received: 8 June 2024
Revised: 24 June 2024
Accepted: 27 June 2024
Published: 1 July 2024

1. Introduction

The disc-stack centrifuge is a highly efficient separation equipment [1–4] that completes the separation using a high-speed rotating drum part, which has a multi-layer disc combination inside the drum to form a separation channel. The liquid in the separation channel under the action of the high-speed rotation of the drum generates a strong centrifugal force field, allowing two different densities and immiscible liquids as well as a small number of fine solid particles to obtain different centrifugal forces, thus achieving liquid-liquid separation, solid-liquid separation, or solid-liquid-liquid separation for separation in the separation channel of the drum [4–8]. The disc-stack centrifuge has the advantages of continuous work, high separation efficiency, strong environmental adaptability, space-saving, and so on [9,10]. Internationally, disc-stack centrifuges are widely used in oil-water separation on ships. In addition, disc-stack centrifuges are commonly used in biopharmaceutical, food processing, petrochemical, environmental protection, and other

fields [11–15]. Among them, the centripetal pump is the key component in the disc-stack centrifuge located at the top of the drum, which converts the kinetic energy of the fluid rotating at high speed into pressure potential energy. It increases the transport pressure of the fluid and discharges the separated liquid out of the disc-stack centrifuge [16]. The centripetal pump plays a vital role as an energy conversion device [17], and its stable working range and total pressure recovery ability have an important impact on the overall efficiency and stability of the disc-stack centrifuge.

The internal flow characteristics of a centripetal pump are intrinsically important indicators of its superior performance. The operating parameters of centripetal pumps seriously affect the internal flow characteristics, which in turn affect the performance of centripetal pumps. The flow inside the centripetal pump is highly complex, and vortices are easily formed in the flow channel, leading to phenomena such as backflow and strong turbulence. Centrifugal and turbine pumps, as conventional radial turbomachines, need to absorb external energy to work on the fluid, and their internal flow characteristics and energy properties are largely known and widely discussed [18–21]. In contrast, very little research has been conducted on unconventional radial turbomachinery where energy conversion is the main feature. In the middle of the 21st century, the study of unconventional radial turbomachinery was initiated, and to date, very little information has been publicly shown on the study of the internal flow characteristics of centripetal pumps. Shen et al. [22] used a combination of numerical simulations and experiments to study and analyze the flow field inside the centripetal pump and to improve the structure of the flow passage to achieve the best performance of the centripetal pump. Sekavčnik et al. [23] used a combination of experimental and numerical simulations to investigate the operating characteristics of a single-stage centripetal pump. It was shown that the inflow conditions to the impeller-stator assembly considerably influenced the flow rate of the stall cessation, the size of the hysteresis, and the head generated during part-load operations. Liu [24] derived the circumferential and absolute velocities of the fluid and determined the trajectory of the fluid based on the continuity equation of the fluid inside the centripetal pump and the law of conservation of angular momentum. The above studies have shown that the flow characteristics inside the flow channel of a centripetal pump directly affect the performance of the centripetal pump.

Additionally, gas-liquid two-phase flow in pumps is a common phenomenon that can seriously destabilize the flow field due to the instability of the gas-liquid interface and has, therefore, attracted a great deal of attention from many researchers and engineers in the pump field. Lomakin et al. [25] used the VOF method to calculate the gas-liquid two-phase flow in a pump. By changing the heights of various initial liquid surfaces in the pump, they studied the effect of the liquid surface height on the internal flow field and established a numerical flow model. Parikh et al. [26] modeled a centrifugal pump using a VOF model for a three-dimensional transient gas-liquid two-phase simulation and confirmed that the use of an inducer and an increase in the lobe-top clearance led to a reduction in the size of the bubbles in the centrifugal pump, as well as a reduction in the range of bubble distribution. Pineda et al. [27] calculated the effect of the void fraction at the inlet of an electric submersible pump on the pump using the VOF method, and the results showed that the dispersion of the void fraction was larger at higher rotational speeds. On the other hand, the pressure head developed decreases as the gas flow rate increases and the inlet pressure decreases. Liu et al. [28] numerically calculated the gas-liquid two-phase flow in a vane pump using MUSIG, an improved model of the VOF method, and found that the area of the low-pressure region in the flow channel near the suction surface of the vane increases gradually with the increase of the volume fraction of the inlet gas and that the gas phase is mainly aggregated in the suction surface of the vane and the wake region, and that the average diameter of the gas bubbles at each place in the pump is closely related to the area of the region of the high gas-phase volume fraction. Luo et al. [29] investigated the centrifugal pump impeller in the gas-liquid two-phase flow field with uneven pressure field by using the SST turbulence model combined with the VOF model and found that

the different locations of gas-liquid two-phase distribution inside the impeller is the main reason for uneven pressure distribution inside the impeller. The above studies have shown that most researchers have used the VOF model for the numerical simulation of gas-liquid two-phase flow in pumps. Combined with the structural characteristics of the centripetal pump, the VOF model is selected as the gas-liquid multiphase flow model in this paper. To improve the accuracy of the numerical simulation, the Mixture model is adopted to carry out the gas-liquid interphase transfer [30].

However, the flow characteristics of a centripetal pump influenced by the operating parameters have not yet been elaborated upon. It is, therefore, necessary to explore the effect of the operating parameters on the internal flow characteristics of centripetal pumps to guide the structural design and optimization of centripetal pumps to achieve optimal performance. In this paper, for a high-parameter, large-capacity centripetal pump model, the VOF/Mixture multiphase flow model is used to study the gas-liquid two-phase flow of the centripetal pump under various working conditions and to explore the working characteristics and two-phase flow mechanism of the centripetal pump, with a focus on the gas-liquid two-phase interfacial position and the total pressure recovery coefficient of the impeller as the two parameters. The gas-liquid interface position determines the stable working range of the centripetal pump, and the total pressure recovery coefficient characterizes the performance of the centripetal pump.

This paper is organized as follows. In Section 2, the geometry and operating principle of the centripetal pump are described, and a reasonable numerical simulation method is determined, including numerical equations, mesh process, and boundary conditions. In Section 3, the variation in the total pressure recovery coefficient and free liquid radius of the centripetal pump for various fuel flows, outlet fuel discharge pressures, and rotation speeds, and the characteristics of the centripetal pump operating characteristics as affected by the operating conditions are derived and discussed. Finally, the conclusions of this study are presented in Section 4.

2. Physical Models and Numerical Simulation

2.1. Model and Meshing

In this paper, the centripetal pump of a disc-stack centrifuge is studied, as shown in Figure 1. Among them, Figure 1a is a schematic diagram of the position of the centripetal pump in a disc-stack centrifuge, Figure 1b is the front view of the centripetal pump structure, the red area is the inlet of the centripetal pump with a total of six inlets, and the black area is the outlet of the centripetal pump, and Figure 1c is an upward view of the I-I position of the centripetal pump, and the green area is the position of the centripetal pump flow channels with a total of six flow channels. The main parameters of the centripetal pump are listed as follows: Q_d is the design flow, N_d is the design rotational speed, and $P_{outlet,d}$ is the design outlet fuel discharge pressure.

According to the centripetal pump solid model, UG NX 12.0 software is used to establish the fluid domain model; as shown in Figure 2, the yellow area is the lower seal, the green area is the upper seal, the pink area is the wall of the centripetal pump room, the blue area is the centripetal pump, the cyan area is the oil discharge pipe, and the purple area is the outlet.

When the centripetal pump works, the upper seal, the lower seal, and the wall of the centripetal pump room rotate at a fixed rotational speed, and the rest is stationary, and the liquid in the centripetal pump room enters the centripetal pump inlet, and is discharged through the oil discharge pipe. The centripetal pump design working conditions with the internal gas-liquid movement pattern are shown in Figure 3; red for liquid and blue for gas.

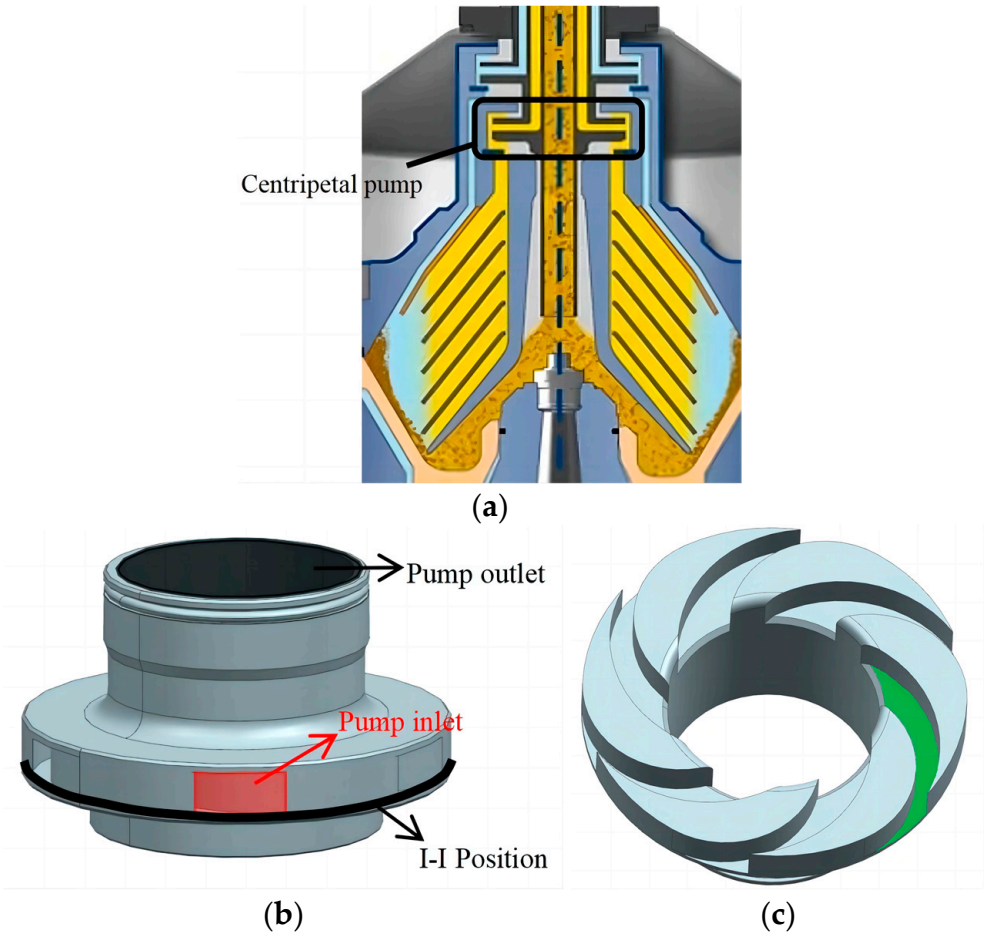

Figure 1. Disc-stack centrifuge and centripetal pump. (**a**) Sectional view of the disc-stack centrifuge. (**b**) Model of the centripetal pump. (**c**) Upward view of the I-I position.

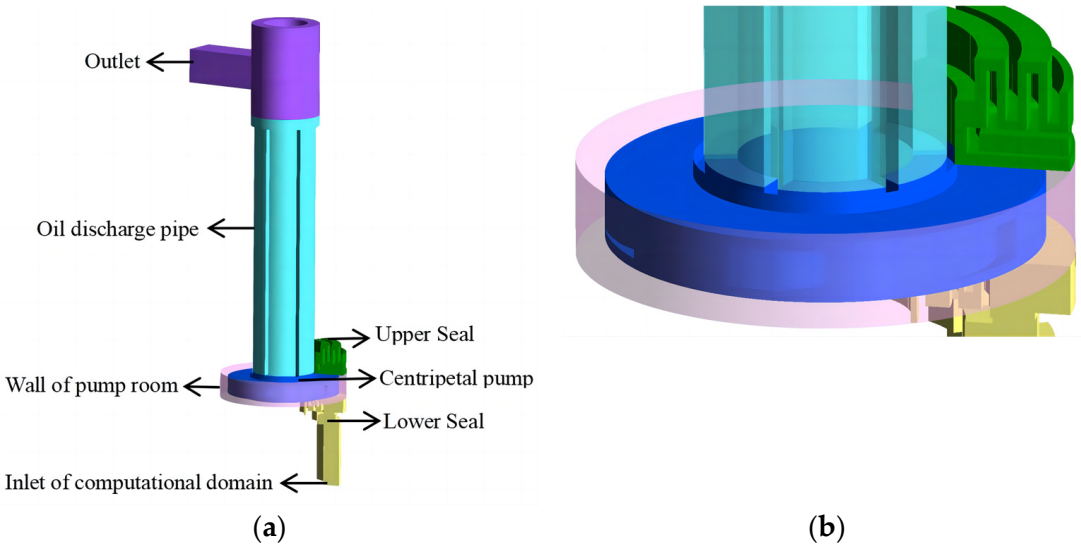

Figure 2. Fluid domain model. (**a**) Fluid domain model. (**b**) Local fluid domain model.

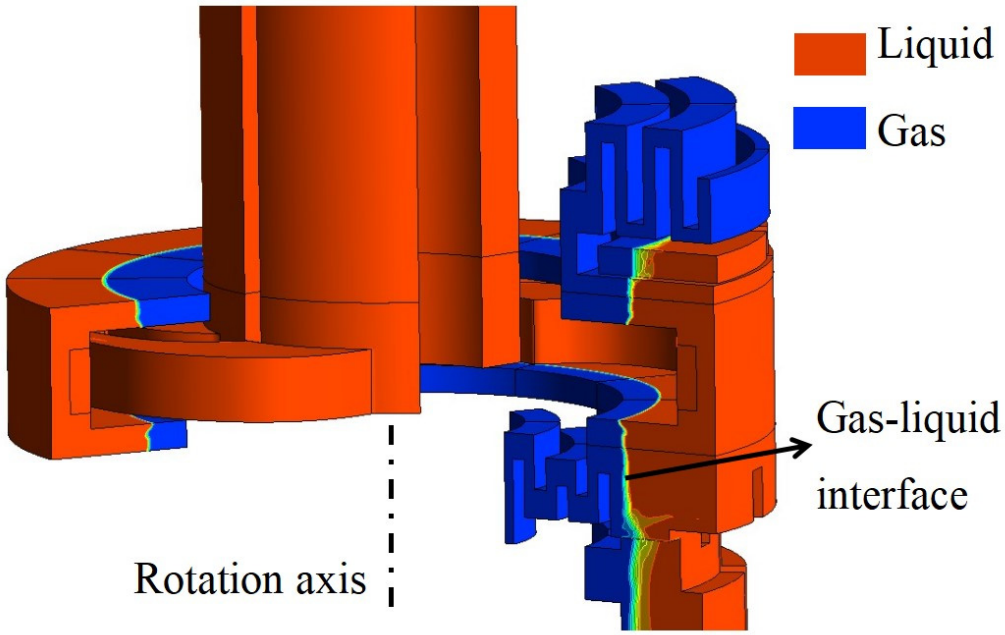

Figure 3. The gas-liquid motion of the centripetal pump.

To evaluate the efficiency of centripetal pumps, the concept of the total pressure recovery coefficient σ is introduced, as shown in Equation (1):

$$\sigma = \frac{P^*_{out}}{P^*_{in}} \tag{1}$$

where σ is a dimensionless parameter, P^*_{in} denotes the average total pressure at the inlet of the centripetal pump flow channels, the unit is MPa and P^*_{out} represents the average total pressure at the outlet of the centripetal pump flow channels, the unit is MPa.

The centripetal pump structure exhibits rotational periodicity, assuming that the flow in each flow channel is the same, the periodicity condition is used to reduce the computational model, the flow channels are 6, the 60° sector of the centripetal pump is used as the computational model, the outlet does not have a symmetric structure, and the full circumference model is used. The structured meshing of the computational domain is performed using ICEM CFD 2021 R1. To study the flow characteristics within the centripetal pump flow channel, the mesh of the flow channel is locally encrypted, and the Y Plus < 30 in the near-wall region of the mesh meets the requirements of the RNG k-ε turbulence model. Figure 4 shows the overall mesh layout of the computational domain and the local area mesh details. Using this gridding method, the computational requirements can be met, and the flow details in the centripetal pump flow channel can be captured.

To ensure the accuracy of numerical simulation, the computational domain is divided into five sets of grids; the number of grids is 340 thousand, 490 thousand, 740 thousand, 1.12 million, and 1.6 million, respectively. The grid independence of the computational domain is verified by using the VOF/Mixture multiphase flow model. Figure 5 shows the variation in the total pressure recovery coefficient of the centripetal pump with the number of grids under the design conditions. The total pressure recovery coefficient represents the performance of the centripetal pump when the total number of grids exceeds 740 thousand; the variation in the total pressure recovery coefficient of the centripetal pump is less than 0.3%, so a grid of 740 thousand is chosen as the calculation model.

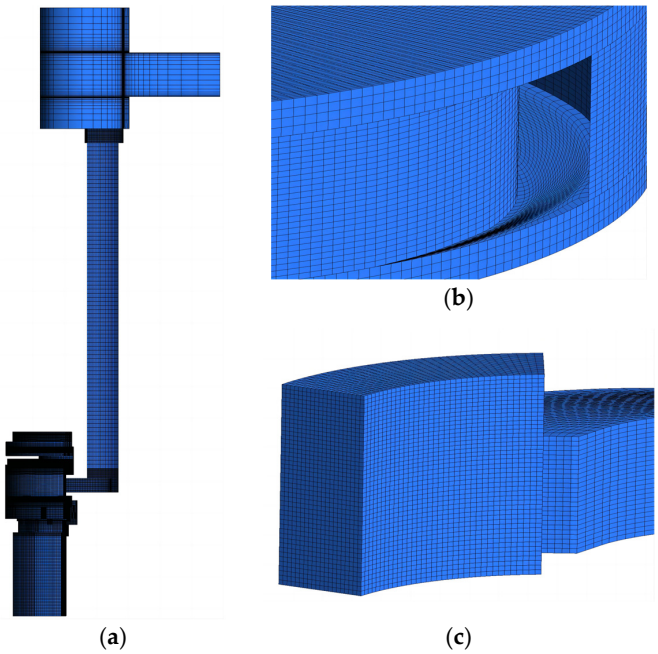

Figure 4. Mesh of the centripetal pump. (**a**) Computational model mesh. (**b**) Mesh at the inlet of a centripetal pump. (**c**) Mesh at the outlet of a centripetal pump.

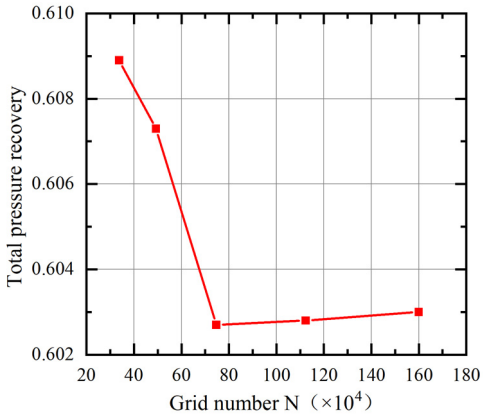

Figure 5. Mesh independence analysis for numerical simulation.

2.2. Numerical Methods and Boundary Conditions

In this paper, based on the ANSYS CFX 2021 R1 software, the VOF/Mixture multiphase flow model is used to numerically simulate the steady-state flow field of the centripetal pump. Based on the consideration of the physical phenomena of the fluid, the simplification of the special problems, and the requirement of the simulation accuracy, the *RNG* k- epsilon turbulence model is selected, and the Total Energy model is used as the heat transfer homogenization model, with an inlet turbulence degree of 5%, and the viscous heating is considered. The computational domain medium is set to be fuel and air, with velocity inlet boundary conditions, 100% inlet oil content and a total fluid temperature of 288.15 K. Pressure outlet boundary conditions were used at the exit, and open boundary conditions were used at both the upper and lower seals, the medium at the seals was air, the relative pressure at the lower seal was 0 Pa, and the pressure at the upper seal was determined by the heavy-phase liquid in disc-stack centrifuge. If fuel flows out of the upper seal outlet, the centripetal pump is leaking and not working properly. A monitoring point is set up during the numerical simulation to monitor the flow at the upper seal outlet, and if liquid flows out of the upper seal outlet after the calculation has converged, the centripetal pump is

judged to be leaking, and it cannot work normally under this condition, and the numerical simulation is terminated.

3. Results and Discussion

To analyze the effects of fuel flow, rotational speed, and outlet fuel discharge pressure on the centripetal pump, the flow coefficient Q_h of the centripetal pump is defined as follows:

$$Q_h = \frac{Q}{Q_d} \tag{2}$$

In the equation, Q_h is a dimensionless parameter, Q is the actual flow of the centripetal pump, the unit is m^3/h, and Q_d is the design flow of the centripetal pump, the unit is m^3/h.

The rotational speed coefficient N_h is as follows:

$$N_h = \frac{N}{N_d} \tag{3}$$

In the equation, N_h is a dimensionless parameter, N is the actual rotational speed of the centripetal pump, unit is rpm, and N_d is the design rotational speed of the centripetal pump, unit is rpm.

The outlet fuel discharge pressure coefficient $P_{outlet,h}$ is as follows:

$$P_{outlet,h} = \frac{P_{outlet}}{P_{outlet,d}} \tag{4}$$

In the equation, $P_{outlet,h}$ is a dimensionless parameter, P_{outlet} is the actual outlet fuel discharge pressure of the centripetal pump, the unit is MPa and $P_{outlet,d}$ is the design outlet fuel discharge pressure of the centripetal pump, the unit is MPa.

To evaluate the flow of the centripetal pump flow channels, the concept of the flow channels flow coefficient C is defined as follows:

$$C = \frac{M}{M_{th}} = \frac{L \times H}{L_{th} \times H_{th}} \tag{5}$$

In the equation, C is a dimensionless parameter, M is the minimum effective flow area at any cross-section in the flow channels, unit is m^2, M_{th} is the effective flow area at the throat cross-section in the flow channels, unit is m^2, L is the minimum effective flow width at any cross-section in the flow channels, unit is m, L_{th} is the effective flow width at the throat cross-section in the flow channels, unit is m, H is the flow channels height at any cross-section in the flow channels, unit is m, and H_{th} is the flow channels height at the throat cross-section, unit is m, $H = H_{th}$, as shown in Figure 6.

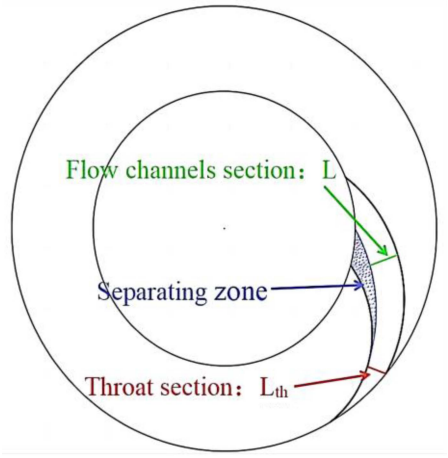

Figure 6. Schematic diagram of flow channel cross-section.

3.1. Fuel Flow Impact Analysis

Figure 7 shows the effect of the outlet fuel discharge pressure and fuel flow on the radius of the free surface and the total pressure recovery capacity of the centripetal pump at the design rotational speed. It can be seen that at the design rotational speed, when $Q_h < 1$, the free surface radius increases with increasing flow. When $Q_h > 1$, the free surface radius decreases with increasing flow, and the maximum point of the free surface radius occurs at the design fuel flow. In the range of Q_h = 0.9~1.2, the normal operating outlet fuel discharge pressure of the centripetal pump is $P_{outlet,h}$ = 0.92~1.28, indicating that the flow has a small effect on the operating pressure range of the centripetal pump. The total pressure recovery coefficient increases with increasing flow; at $Q_h > 1$, the rate of change of the total pressure recovery coefficient is small, and when the flow coefficient is increased by 1, the total pressure recovery coefficient increases by 0.1. at $Q_h < 1$, the rate of change of the total pressure recovery coefficient is about five times that at $Q_h > 1$.

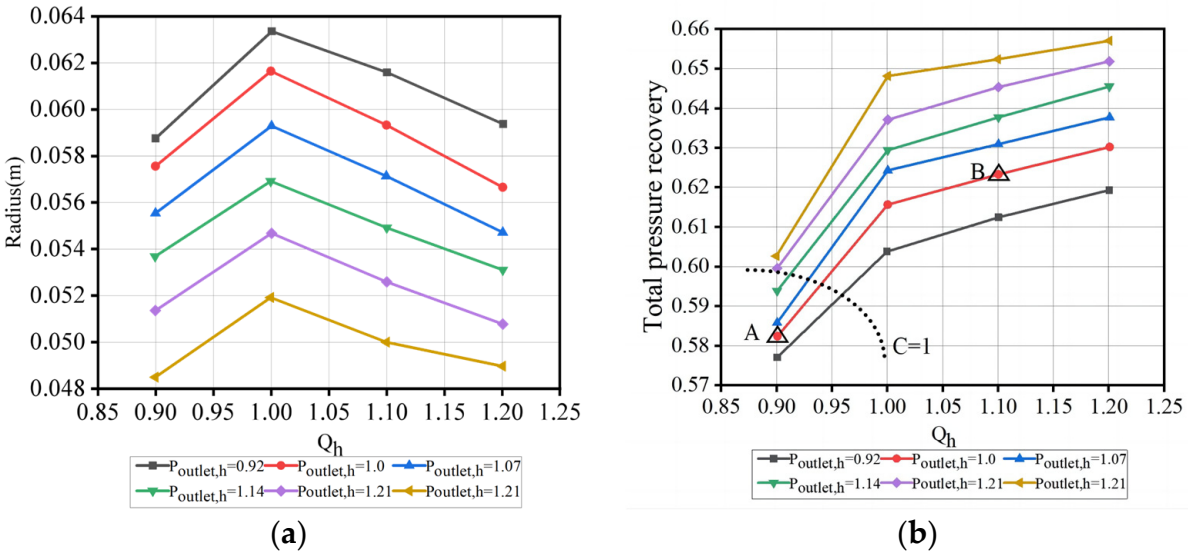

Figure 7. Working characteristics of centripetal pumps at different design speeds. (**a**) Change in radius of the free liquid surface. (**b**) Change in the total pressure coefficient of restitution.

Take the centripetal pump flow path 50% spanwise position flow surface to analyze, with the design rotational speed, design outlet fuel discharge pressure, compare Q_h = 0.9, Q_h = 1.1 two conditions flow surface velocity distribution, as shown in Figure 8. It can be seen that at Q_h = 0.9, the area of the separation zone on the suction side of the centripetal pump flow channel is larger, indicating that the fluid is seriously separated here and blocks the flow channel, where $L = 0.75L_{th}$, i.e., C = 0.75; corresponding to point A in Figure 7b, the total pressure recovery coefficient is low. In addition, with increasing flow, the flow separation initiation point moves downstream, and the area of the separation zone decreases, where $L = 1.5L_{th}$, i.e., C = 1.5, at Q_h = 1.1, corresponds to point B in Figure 7b. In summary, the total pressure recovery coefficient of the centripetal pump is closely related to the effective flow area in the flow channel, and the flow increase is favorable to suppress the flow separation.

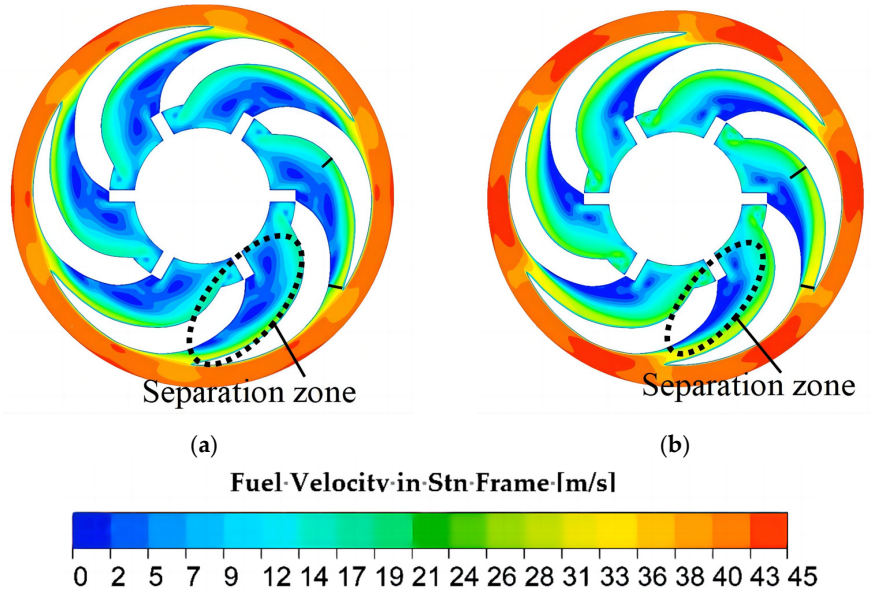

Figure 8. Velocity distribution. (**a**) Q_h = 0.9. (**b**) Q_h = 1.1.

3.2. Outlet Fuel Discharge Pressure Impact Analysis

The effects of outlet fuel discharge pressure and flow on the radius of the free liquid surface and the total pressure recovery capacity of centripetal pumps at the design rotational speed are shown in Figure 9. The outlet fuel discharge pressure decreases until the fuel leaks from the upper seal. It can be seen that the radius of the free liquid surface decreases gradually with the outlet fuel discharge pressure at the design rotational speed, and the rate of change of the radius of the free liquid surface remains the same. Meanwhile, the total pressure recovery coefficient increases gradually with the outlet fuel discharge pressure, and the change is quantitatively smooth. When the outlet fuel discharge pressure coefficient $P_{outlet,h}$ is increased by 1, the total pressure recovery coefficient increased by 0.067.

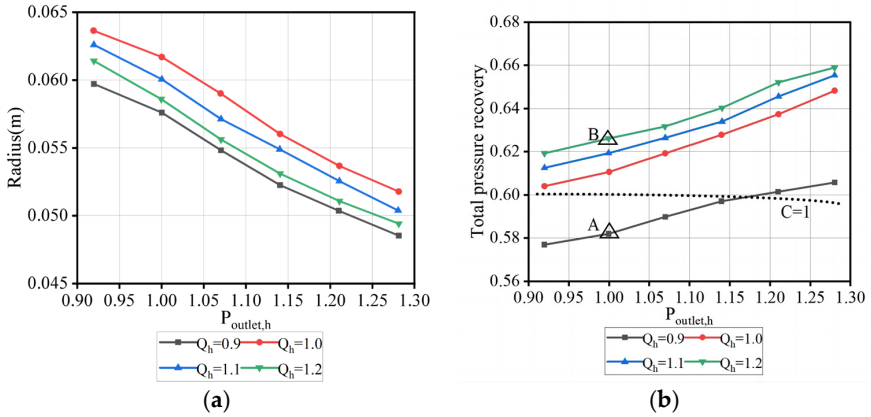

Figure 9. Working characteristics of centripetal pumps at design speeds. (**a**) Change in radius of free liquid surface. (**b**) Change in total pressure coefficient of restitution.

During the normal operation of the centripetal pumps, the resistance loss along the flow channel varies less with the outlet fuel discharge pressure, and the pressure at the inlet of the flow channel of the centripetal pumps increases with an increase in the outlet fuel discharge pressure, as shown in Figure 10. The centrifugal hydraulic pressure difference at the free liquid surface and the inlet of the flow channel P is:

$$P = \rho\omega^2\left(r^2 - r_f^2\right) \tag{6}$$

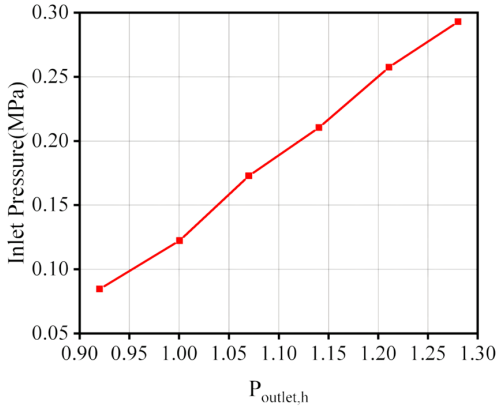

Figure 10. Centripetal pump inlet pressure change.

In the equation, the unit of P is Pa, ρ is the density of the liquid, the unit is kg/m^3, ω is the rotational speed of the liquid, the unit is rps, r is the radius of the inlet of the flow channel of the centripetal pump, the unit is m, and r_f is the radius of the free liquid surface unit is m.

From the working principle of the centripetal pump and Equation (6), it can be seen that as the pressure at the inlet of the flow channel of the centripetal pumps increases, the free liquid surface moves toward the sealing outlet, i.e., the higher the outlet fuel discharge pressure, the smaller the radius of the free liquid surface.

Take the centripetal pump flow channel 50% spanwise position flow surface to analyze velocity distributions of Q_h = 0.9 and Q_h = 1.2; conditions are compared at the design rotational speed and design outlet fuel discharge pressure, two conditions velocity distribution, as shown in Figure 11. It can be seen that when Q_h = 0.9, the centripetal pump flow channel suction side of the separation zone area is larger, indicating that the fluid in this place undergoes serious separation, blocking the flow channel. At this time, $L = 0.75L_{th}$, i.e., C = 0.75, corresponding to point A in Figure 9b, the total pressure recovery coefficient is low. When Q_h = 1.2, the area of the separation zone area on the suction side of the flow channel of the centripetal pump is smaller, and the starting point of flow separation moves downstream, at this time, $L = 1.5L_{th}$, i.e., C = 0.75; corresponding to the point B of Figure 9b.

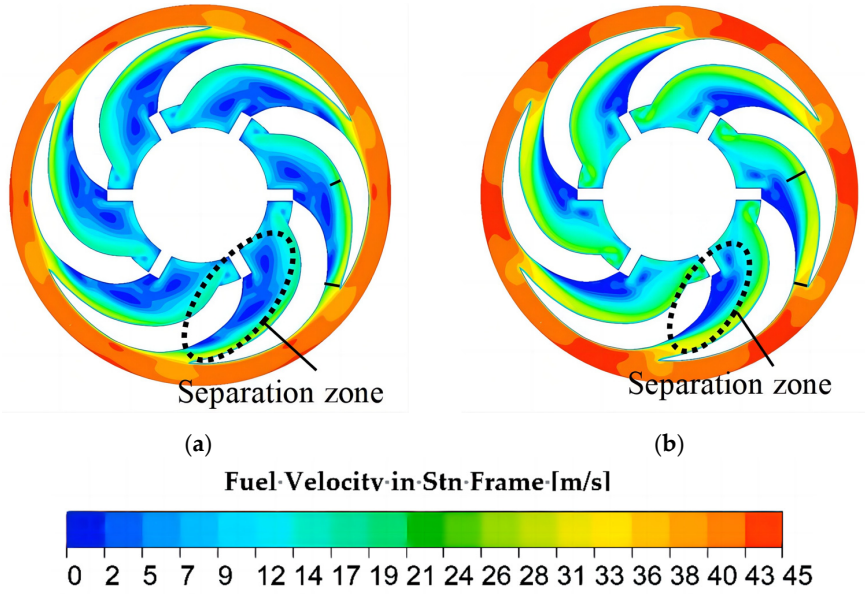

Figure 11. Velocity distribution. (**a**) $_{Qh}$ = 0.9. (**b**) Q_h = 1.2.

3.3. Rotational Speed Impact Analysis

Figure 12 shows the effect of flow and rotational speed on the radius of the free surface and the total pressure recovery of a centripetal pump at 1.21 times the design outlet fuel discharge pressure. When N_h = 0.9, all the flow conditions leak the fuel and do not work properly. It can be seen that when $P_{outlet,h}$ = 1.21, the radius of the free liquid surface increases gradually with the rotational speed, and when the rotational speed coefficient N_h increases by 1, the radius of the free liquid surface increases by 0.075 m. The total pressure recovery coefficient decreases gradually with rotational speed, and when Q_h = 1.1~1.2, it varies uniformly with rotational speed, and when Q_h = 0.9~1.0, the total pressure recovery coefficient decreases sharply when N_h = 1.06, which the change in centripetal pump performance is especially obvious at N_h = 1.06, Q_h = 1.0.

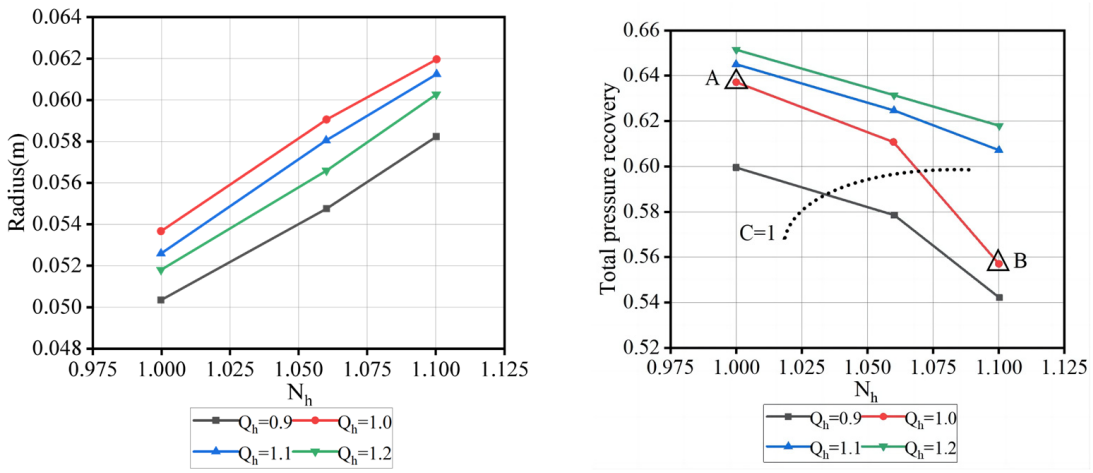

(**a**) (**b**)

Figure 12. Centripetal pump working characteristics at 1.21 the fuel design discharge pressure. (**a**) Change in radius of the free liquid surface. (**b**) Change in the total pressure coefficient of restitution.

When only changing the rotational speed, the circumferential velocity of the fluid entering the flow channel of the centripetal pump increases with the rotational speed. From the theoretical analysis, it can be seen that when the flow and pressure are constant, the total pressure in the pump is unchanged, and with the increase in rotational speed, the centrifugal inertia acceleration increases. The larger the inlet dynamic pressure, the smaller the static pressure, and therefore, the radius of the free surface of the liquid increases.

Take the centripetal pump flow channel 50% spanwise position flow surface to analyze, with the design fuel flow, 1.21 times the design outlet fuel discharge pressure, comparing the N_h = 1.0 and N_h = 1.1 two conditions velocity distribution, as shown in Figure 13. It can be seen that when N_h = 1.0, the area of the separation zone on the suction side of the centripetal pump flow channel is smaller; at this time, $L = 1.2L_{th}$, i.e., C = 1.2, corresponds to point A in Figure 12b. When N_h = 1.1, the centripetal pump flow channel suction side of the low-velocity area is larger, indicating that the fluid in this place undergoes serious separation, blocking the flow channel; at this time, $L = 0.8L_{th}$, i.e., C = 0.8, corresponds to point B in Figure 12b, and the total pressure recovery coefficient is low. In summary, the low-speed operation of centripetal pumps is conducive to suppressing the flow separation and maintaining a large effective flow area in the flow channel.

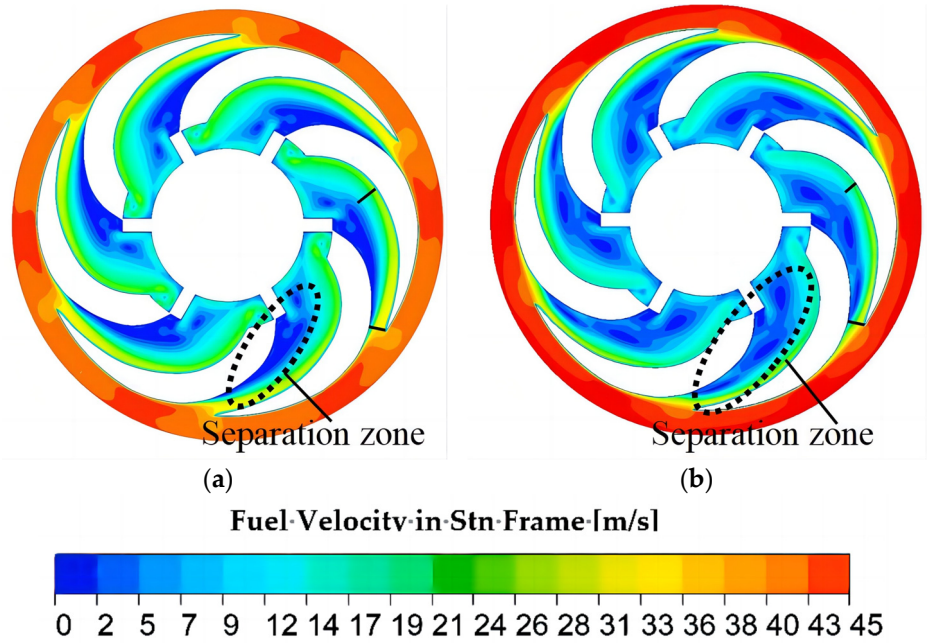

Figure 13. Velocity distribution. (**a**) N_h = 1.0. (**b**) N_h = 1.1.

3.4. Centripetal Pump Unsteady Working State

As can be seen from Figures 7 and 8, when $Q_h < 1$, i.e., small flow coefficient, the area of the separation zone in the flow channel is larger, blocking the flow channel, the flow channel flow coefficient $C < 1$, the total pressure recovery capacity is small, and the radius of the free liquid surface increases with the increase in flow.

As can be seen from Figures 9 and 11, it can be seen that the outlet fuel discharge pressure has less influence on the working condition of the centripetal pump, and the total pressure recovery coefficient of the centripetal pump varies in a small range with the outlet fuel discharge pressure; when $Q_h < 1$, the area of the separation zone in the flow channel is larger, blocking the flow channel, the flow channel flow coefficient $C < 1$, and the total pressure recovery ability is small, and the radius of the free liquid surface increases with the increase of flow.

As shown in Figures 12 and 13, when $N_h > 1.06$, i.e., a large rotational speed coefficient, the area of the separation zone in the flow channel is larger, blocking the flow channel. When the flow channel flow coefficient $C < 1$, the total pressure recovery capacity is small, and the radius of the free liquid surface increases with the flow. This situation only occurs in the $Q_h \leq 1$ condition.

In summary, this paper will be about centripetal pump flow channel flow coefficient $C < 1$, the total pressure recovery coefficient is small, and the free liquid surface radius increases with an increase in flow, which is called an unsteady working state. Moreover, an unsteady working state is likely to occur at low flow coefficients and high rotational speed coefficients. After the centripetal pump enters the unsteady working condition, the total pressure recovery coefficient of the centripetal pump decreases significantly, the flow capacity of the centripetal pump deteriorates due to the serious flow separation phenomenon, and the vibration and noise phenomena are intensified. Therefore, it is recommended that centripetal pumps be operated at low rotational speed coefficients and high flow coefficients.

3.5. Transition Mechanisms between Steady and Unsteady Working State

From the analysis of Figures 8, 11, and 13, it can be seen that the working state of the centripetal pump is determined by the flow coefficient of the flow channel. When the flow coefficient $C > 1$, the centripetal pump is in a steady working state, and the separation area in the centripetal pump flow channel is small. When the flow coefficient $C < 1$, the

centripetal pump is in an unsteady working state, and the separation area in the flow channel of the centripetal pump is large. It is because there is an adverse pressure gradient along the flow direction in the flow channel of the centripetal pump, i.e., the fluid is flowing under the adverse pressure gradient, and thus the velocity decreases rapidly. On the other hand, when the fluid flows along the wall, the thickness of the boundary layer gradually increases, and due to the viscous friction effect, there is a great loss of fluid kinetic energy near the wall. Under this double action, the fluid flow stops at a certain point on the suction surface of the flow channel, and the fluid inside the boundary layer after this point undergoes a backflow phenomenon under the action of an adverse pressure gradient. The point is called the separation point; after the separation point, the fluid in the separation zone forms a vortex. When the centripetal pump is in a steady working condition, the centripetal pump flow channel inside the adverse pressure gradient rate of change is small; that is, along the flow direction, the pressure growth in the flow channel is flat, delayed occurrence of the separation phenomenon, the separation point is far from the inlet of the flow channel, the separation zone area is small.

The phenomenon is consistent with the theoretical derivation, indicating that the results of the numerical simulation are reliable. It fills a gap in the study of the working characteristics of centripetal pumps and the flow law in the flow channel.

The most important factor in determining the working condition of the centripetal pump is the size of the separation area within the flow channel of the centripetal pump. When the curvature of the flow channel of the centripetal pump is large along the direction of the flow, the greater the rate of change of the fluid adverse pressure gradient, the flow within the centripetal pump is more prone to reflux phenomena, resulting in separation. Changing the curvature of the flow channel of the centripetal pump can change the rate of change of the adverse pressure gradient in the flow channel of the centripetal pump. When the curvature of the flow channel of the centripetal pump is small along the direction of the flow, the rate of change of the adverse pressure gradient is low, and it is not easy to separate the flow in the flow channel of the centripetal pump, which will make the total pressure recovery coefficient of the centripetal pump increase.

4. Conclusions

(1) In the steady working state, the radius of the free liquid surface of the gas-liquid two-phase centripetal pump decreases with an increase in inlet fuel flow, decreases with an increase in outlet fuel discharge pressure, and increases with an increase in rotational speed. When the speed coefficient increases by 1, the radius of the free liquid surface increases by 0.075 m. The gas-liquid two-phase free liquid surface of the centripetal pump fluctuates in the range of 0.048 m to 0.068 m during the process of calculation simulation.

(2) In the steady working state, the total pressure recovery coefficient of the centripetal pump increases with an increase in the fuel flow. When the flow coefficient is increased by 1, the total pressure recovery coefficient increases by 0.1. The total pressure recovery coefficient of the centripetal pump increases with an increase in the outlet fuel discharge pressure. When the fuel discharge pressure coefficient is increased by 1, the total pressure recovery coefficient increases by 0.067. The total pressure recovery coefficient of the centripetal pump decreases with an increase in the rotational speed. The total pressure recovery coefficient of the centripetal pump fluctuates in the range of 0.57~0.67 during the calculation simulation.

(3) There is an unsteady working state of the centripetal pump, that is, in the high-speed coefficient, small flow coefficient conditions, centripetal pump flow channel flow, there is a large-scale separation phenomenon, blocking the flow channel, flow channel flow coefficient $C < 1$, the total pressure recovery capacity $\sigma < 0.6$. As the rotational speed reduction or fuel flow increases, the centripetal pump flow channel separation area decreases, the flow channel flow coefficient C gradually increases, and the centripetal pump tends to stabilize the working state.

(4) Changing the curvature of the flow channel of the centripetal pump can change the rate of change of the adverse pressure gradient in the flow channel of the centripetal pump when the curvature of the flow channel of the centripetal pump is small along the direction of the flow, the rate of change of the adverse pressure gradient is small, and it is not easy to separate the flow in the flow channel of the centripetal pump, which will make the total pressure recovery coefficient of the centripetal pump increase.

Author Contributions: Writing—original draft preparation, methodology, validation, S.L. (Shoulie Liu); investigation, H.D.; conceptualization, writing-review and editing, S.L. (Shaobin Li); validation, X.S. All authors have read and agreed to the published version of the manuscript.

Funding: This research received no external funding.

Data Availability Statement: The original contributions presented in the study are included in the article, further inquiries can be directed to the corresponding author.

Conflicts of Interest: Author Hefeng Dong was employed by the company China State Shipbuilding Corporation Limited. The remaining authors declare that the research was conducted in the absence of any commercial or financial relationships that could be construed as a potential conflict of interest. The company had no role in the design of the study; in the collection, analyses, or interpretation of data; in the writing of the manuscript, or in the decision to publish the results.

Nomenclature

σ	Total pressure recovery coefficient of the centripetal pump
P_{out}*	Average total pressure at the outlet of the centripetal pump flow channels (MPa)
P_{in}*	Average total pressure at the inlet of the centripetal pump flow channels (MPa)
Q_h	Flow coefficient of the centripetal pump
Q	Actual flow of the centripetal pump (m^3/h)
Q_d	Design flow of the centripetal pump (m^3/h)
N_h	Speed coefficient of the centripetal pump
N	Actual rotational speed of the centripetal pump (rpm)
N_d	Design rotational speed of the centripetal pump (rpm)
$P_{outlet,h}$	Outlet fuel discharge pressure coefficient
P_{outlet}	Actual outlet fuel discharge pressure of the centripetal pump (MPa)
$P_{outlet,d}$	Design outlet fuel discharge pressure of the centripetal pump (MPa)
C	Flow channels flow coefficient of the centripetal pump
M	Minimum effective flow area at any cross-section in the flow channels (m^2)
M_{th}	Effective flow area at the throat cross-section in the flow channels (m^2)
L	Minimum effective flow width at any cross-section in the flow channels (m)
L_{th}	effective flow width at the throat cross-section in the flow channels (m)
H	flow channels height at any cross-section in the flow channels (m)
H_{th}	flow channels height at the throat cross-section in the flow channels (m)
P	centrifugal hydraulic pressure difference at the free liquid surface and the inlet of the flow channel (Pa)
ρ	Density of the liquid in centripetal pump (kg/m^3)
ω	Rotational speed of the liquid in centripetal pump (rps)
r	Radius of the inlet of the flow channel of the centripetal pump (m)
r_f	Radius of the free liquid surface in centripetal pump (m)

References

1. Yuan, H. *Separation Engineering*; China Petrochemical Press: Beijing, China, 2002; pp. 113–115.
2. Sun, Q.; Jin, D. *Centrifuge Principle Structure and Design Calculation*; China Machine Press: Beijing, China, 1987; pp. 530–533.
3. Ahranjani, P.E.; Hajimoradi, M. Optimization of industrial-scale centrifugal separation of biological products: Comparing the performance of tubular and disc stack centrifuges. *Biochem. Eng. J.* **2022**, *178*, 108281.
4. Agrell, J.; Faucher, M.S. Recovery of Heavy Oil and Bitumen Using Disc-Stack Centrifuge Technology. In Proceedings of the SPE International Thermal Operations and Heavy Oil Symposium, Calgary, AB, Canada, 1–3 November 2005.

5. Szepessy, S.; Thorwid, P. Low Energy Consumption of High-Speed Centrifuges. *Chem. Eng. Technol.* **2018**, *41*, 2375–2384. [CrossRef]
6. Wang, H.; Li, B.; Lai, D. Fluid simulation analysis of centripetal pump for disc separator. *Filtrat. Separat.* **2013**, *23*, 22–25.
7. Zhao, Z. The Influence of Structural Changes on The Interior Flow Field's Characteristics of Disc Separator. *Procedia Eng.* **2011**, *15*, 5051–5055. [CrossRef]
8. Fu, S.; Zhu, J.; Zhou, F.; Yuan, H.; Miao, W. Study on the characteristics of flow field in disc partition in disccentrifuge. *Asia-Pac. J. Chem. Eng.* **2021**, *16*, e2666. [CrossRef]
9. Dhuldhoya, N.; Mileo, M.; Faucher, M.; Sellman, E. Dehydration of Heavy Crude Oil Using Disc Stack Centrifuges. In Proceedings of the SPE Annual Technical Conference and Exhibition, New Orleans, LA, USA, 27–30 September 1998.
10. Agrell, J.; Faucher, M. Heavy Oil and Bitumen Dehydration-A Comparison between Disc-Stack Centrifuges and Conventional Separation Technology. *SPE Prod. Oper.* **2007**, *22*, 156–160. [CrossRef]
11. Yang, M.; Liu, X.; Howell, J.A.; Cheng, H. Analysis and estimation/prediction of the disk stack centrifuge separation performance-Scaling fr-om benchtop fixed rotor type to disk stack centri-fuges. *Sep. Sci. Technol.* **2020**, *55*, 2615–2621. [CrossRef]
12. Shekhawat, L.K.; Sarkar, J.; Gupta, R.; Hadpe, S.; Rathore, A.S. Application of CFD in Bioprocessing: Separation of mammalian cells using disc stack centrifuge during production of biotherapeutics. *J. Biotechnol.* **2018**, *267*, 1–11. [CrossRef]
13. Zhang, Z.; Dong, H.; Wang, R.; Liu, F. Research on Influence Parameters of Separation Performance of Disc Centrifuge. *J. Filtr. Sep.* **2017**, *27*, 17–23.
14. Cambiella, A.; Benito, J.M.; Pazos, C.; Coca, J. Centrifugal separation efficiency in the treatment of waste emulsified oils. *Chem. Eng. Res. Des.* **2006**, *84*, 69–76. [CrossRef]
15. Sun, B.; Gong, J.; Xin, Z.; Zhao, W.Y.; Wu, W.Y.; Wu, J.M. Experimental study on Yellow River's silt separation for drip irrigation. *Trans. CSAE* **2008**, *24*, 51–53.
16. Jin, M. Application of centripetal pump technology in centrifugal separators. *Filtrat. Separat.* **1997**, *39*, 21–24.
17. Zhang, W.; Xie, C.; Wang, L. Exploration of separation technology of disc centrifuge. *Electromech. Equip.* **2018**, *35*, 1–5.
18. Li, W.; Huang, Y.; Ji, L.; Ma, L.; Agarwal, R.K.; Awais, M. Prediction model for energy conversion characteristics during transient processes in a mixed-flow pump. *Energy* **2023**, *271*, 127082. [CrossRef]
19. Suh, J.W.; Kim, J.W.; Choi, Y.S.; Kim, J.H.; Joo, W.G.; Lee, K.Y. Development of numerical Eulerian-Eulerian models for simulating multiphase pumps. *J. Pet. Sci. Eng.* **2018**, *162*, 588–601. [CrossRef]
20. He, D.; Ge, Z.; Bai, B.; Guo, P.; Luo, X. Gas–liquid two-phase performance of centrifugal pump under bubble inflow based on computational fluid dynamics–population balance model coupling model. *J. Fluids Eng.* **2020**, *142*, 081402. [CrossRef]
21. Zhang, N.; Jiang, J.; Gao, B.; Liu, X.; Ni, D. Numerical analysis of the vortical structure and its unsteady evolution of a centrifugal pump. *Renew. Energy* **2020**, *155*, 748–760. [CrossRef]
22. Shen, S.; Zhou, F.; Fu, S.; Hu, Y.; Shen, Z.; Xu, M.; Li, K.; Zhang, S. Optimization and test study of centripetal pump in disc-stack centrifuge based on flow field analysis. *J. Taiwan Inst. Chem. Eng.* **2023**, *153*, 105200. [CrossRef]
23. Sekavčnik, M.; Gantar, T.; Mori, M. A Single-Stage Centripetal Pump-Design Features and an Investigation of the Operating Characteristics. *ASME Fluids Eng.* **2010**, *132*, 021106. [CrossRef]
24. Liu, B. Research on the design of centripetal pumps for disc separators. *Oasis. Technol.* **1993**, *1*, 9–11.
25. Lomakin, V.O.; Kuleshovav, M.S.; Bozh'eva, S.M. Numerical Modeling of Liquid Flow in a Pump Station. *Power Technol. Eng.* **2016**, *49*, 324–327. [CrossRef]
26. Parikh, T.; Mansour, M.; Thévenin, D. Investigations on the effect of tip clearance gap and inducer on the transport of air-water two-phase flow by centrifugal pumps. *Chem. Eng. Sci.* **2020**, *218*, 115554. [CrossRef]
27. Pineda, H.; Biazussi, J.; López, F.; Oliveira, B.; Carvalho, R.D.; Bannwart, A.C.; Ratkovich, N. Phase distribution analysis in an Electrical Submersible Pump (ESP) inlet handling water-air two-phase flow using Computational Fluid Dynamics. *J. Pet. Sci. Eng.* **2016**, *139*, 49–61. [CrossRef]
28. Liu, H.; Du, X.; Wu, X.; Tan, M. Numerical simulation on gas-phase characteristics of gas-liquid two-phase flow in pump. *J. Drain. Irrig. Mach. Eng.* **2022**, *40*, 238–243.
29. Luo, X.; Yan, S.; Feng, J.; Zhu, G.; Sun, S.; Chen, S. Force characteristics of gas-liquid two-phase centrifugal pump. *Trans. Chin. Soc. Agric. Eng.* **2019**, *35*, 66–72.
30. Cheng, X.; Chen, X. Progress in numerical simulation of high entrained air-water two-phase flow. In Proceedings of the 3nd International Conference on Digital Manufacturing & Automation (ICDMA2012), Guilin, China, 31 July–2 August 2012; p. 4.